

High-Molecular-Weight Atactic Polypropylene from Metallocene Catalysts. 1. $\text{Me}_2\text{Si}(\text{9-Flu})_2\text{ZrX}_2$ ($\text{X} = \text{Cl, Me}$)

Luigi Resconi*

Montell Polyolefins, G. Natta Research Center, P.le Donegani 12, 44100 Ferrara, Italy

Robert L. Jones

Montell Polyolefins, Research & Development Center, 912 Appleton Road, Elkton, Maryland 21921

Arnold L. Rheingold and Glenn P. A. Yap

Department of Chemistry, University of Delaware, Newark, Delaware 19716

Received March 14, 1995[⊗]

The synthesis and characterization of the C_{2v} symmetric (dimethylsilanediylbis(9-fluorenyl))zirconium dichloride (**I**) and (dimethylsilanediylbis(9-fluorenyl))zirconium dimethyl (**II**) are reported. The crystal and molecular structure of **II** has been solved. The catalyst system **I**/MAO and **II**/MAO (MAO = methylalumoxane) produce high-molecular-weight atactic polypropylene at relatively high polymerization temperatures ($M_w = (1-4) \times 10^5$ at 50 °C and Al/Zr = 1200) in good yields, providing a practical entry to this novel, elastomeric propylene homopolymer.

Introduction

Group 4 metallocene-based catalysts allow the production of polyolefins in a much wider range of composition and microstructures than any other catalytic systems, thanks to the extraordinary steric and electronic variability of the cyclopentadienyl ligands.

In the case of propylene polymerization, both highly isotactic¹ and highly syndiotactic² polymers have been obtained, as well as practically all intermediate microstructures, including ideally atactic polypropylene.³

The ability to control polymer molecular weight is as important as control over catalyst stereospecificity, as metallocene catalysts tend to produce lower molecular weight poly(α -olefins) than industrial catalysts, especially at practical polymerization temperatures. The fundamental issue of molecular weight control has been solved for both isotactic^{1b,4} and syndiotactic⁵ polypropylenes through modification of the cyclopentadienyl ligand substitution pattern, while until very recently little attention has been dedicated to less or nonstereoregular polymers.⁶

Low-molecular-weight "atactic" polypropylene is obtained as a byproduct in the industrial production of

isotactic polypropylene, finding applications as an additive in bitumens and hot-melt adhesives. This product, however, is actually neither really atactic nor fully amorphous, being a mixture of chains of rather different tacticities and molecular weights.⁷ With the introduction of industrial catalysts having improved stereospecificity, its availability is being reduced, and as a consequence the interest in these amorphous propylene products is rising.

The lack of a direct, high-yield process able to produce atactic polypropylene (aPP) with higher molecular weights has prevented the full investigation of its properties and limited the scope of its applications. Moreover, a positive effect of higher molecular weights and absence of crystallinity on the elastic and optical properties of aPP is apparent.

Our investigation on the direct synthesis of high-molecular-weight aPP resulted in a new zirconocene, the C_{2v} -symmetric (dimethylsilanediylbis(9-fluorenyl))zirconium dichloride (**I**), which is able to produce high-molecular-weight ($M_w > 200\,000$) atactic (fully amorphous) polypropylene at practical (≥ 50 °C) polymerization temperatures.⁸

In this paper we report the synthesis and characterization of **I** and its derivative (dimethylsilanediylbis(9-fluorenyl))zirconium dimethyl (**II**) and the crystal and

[⊗] Abstract published in *Advance ACS Abstracts*, December 15, 1995.

(1) See for example: (a) Mise, T.; Miya, S.; Yamazaki, H. *Chem. Lett.* **1989**, 1853–1856. (b) Spaleck, W.; Küber, F.; Winter, A.; Rohrmann, J.; Bachmann, B.; Antberg, M.; Dolle, V.; Paulus, E. *Organometallics* **1994**, *13*, 954–963 and references therein.

(2) Ewen, J. A.; Elder, M. J.; Jones, R. L.; Curtis, S.; Cheng, H. N. In *Catalytic Olefin Polymerization: Studies in Surface Science and Catalysis* Vol. 56; Keii, T., Soga, K., Eds.; Kodansha/Elsevier: Amsterdam, 1990; pp 439–482.

(3) Ewen, J. A. *J. Am. Chem. Soc.* **1984**, *106*, 6355–6364. Kaminsky, W. *Angew. Makromol. Chem.* **1986**, *145/146*, 149–160.

(4) Spaleck, W.; Antberg, M.; Rohrmann, J.; Winter, A.; Bachmann, B.; Kiprof, P.; Behm, J.; Hermann, W. *Angew. Chem., Int. Ed. Engl.* **1992**, *31*, 1347–1350.

(5) Winter, A.; Rohrmann, J.; Antberg, M.; Dolle, V.; Spaleck, W. Eur. Pat. Appl. 387,690 (to Hoechst), 1990. Razavi, A.; Atwood, J. L. *J. Organomet. Chem.* **1993**, *459*, 117–123.

(6) High-molecular-weight atactic polyhexene has been obtained with $\text{Flu}_2\text{ZrMe}_2$ -based catalysts: Siedle, A.; Lamanna, W.; Newmark, R. *Makromol. Chem. Macromol. Symp.* **1993**, *66*, 215–224.

(7) van der Veen, S. *Polypropylene and other polyolefins*; Elsevier: Amsterdam, 1990. Kakugo, M.; Miyatake, T.; Naito, Y.; Mizunuma, K. *Makromol. Chem.* **1989**, *190*, 505. Busico, V.; Corradini, P.; De Martino, L.; Graziano, F.; Iadicco, A. *Makromol. Chem.* **1991**, *192*, 49–57.

(8) Resconi, L.; Jones, R. L. Eur. Pat. Appl. 604908 (to Spherilene), 1994. Resconi, L.; Albizzati, E. Eur. Pat. Appl. 604917 (to Spherilene), 1994. Resconi, L.; Jones, R. L.; Albizzati, E.; Camurati, I.; Piemontesi, F.; Guglielmi, F.; Balbontin, G. *ACS Polymer Prepr.* **1994**, *35* (1), 663–664.

molecular structure of **II** and compare some of the more relevant polymerization results. The properties of this novel propylene polymer will be reported elsewhere.⁹

Results and Discussion

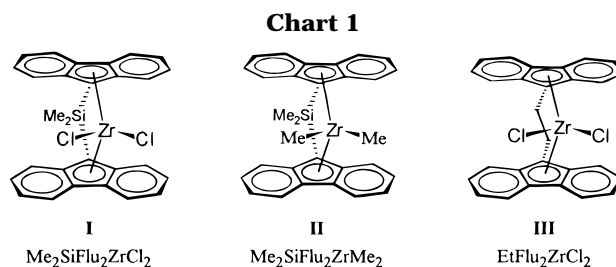
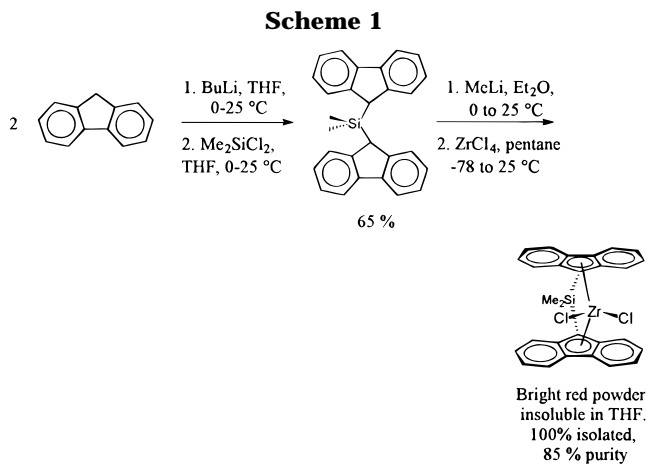
1. Choice of the Ligand. As proven for a new quite large number of metallocene systems, the substitution pattern of the π -Cp ligands affects both propagation rate and type and extent of chain transfer reactions.

In order to increase the polymer molecular weight, one has to design a catalyst with the highest possible propagation rate constant toward monomer insertion and also be able to disfavor sterically the chain conformation leading to chain transfer. It has been reported in the literature that, for chiral, bridged metallocenes, Cp substitution in the positions α to the ligand bridge enhances molecular weight.^{1a,4,10} Silicon-bridged bis(indenyl)zirconocenes produce (isotactic) polypropylene with higher molecular weight with respect to ethylene bridged analogues.¹¹ The fluorenyl group in $\text{Me}_2\text{C}(\text{Cp})(9\text{-Flu})\text{ZrCl}_2$ was observed to favor the production of higher molecular weight (syndiotactic) polypropylenes,² while that in $\text{Flu}_2\text{ZrMe}_2$ gave higher molecular weight atactic polyhexene,⁶ when compared to other metallocene catalysts.

The most common cause for molecular weight depression in metallocene catalysts is β -hydrogen transfer,¹² which can be either monomolecular or bimolecular (chain transfer to the monomer).¹⁰

Our goal was high-molecular-weight *atactic* polypropylene. This would require an *aspecific* C_{2v} -symmetric metallocene as catalyst precursor. During our earlier investigation on the subject, we had found that, for achiral metallocenes,¹³ polymerization activities vary over a wide range and the molecular weight of the propylene products is strongly influenced by the substitution pattern of the two cyclopentadienyl (Cp) ligands.

Molecular model analysis of active centers bearing a polypropylene chain in the conformation leading to β -hydrogen transfer clearly shows that substitution of hydrogens for alkyl groups at the Cp frontal positions (the four β positions in the case of a bridged metallocene) increases the nonbonded interactions between Cp ligand and growing chain, thus increasing the energy required for β -H transfer. The above evidence led us to the synthesis of (dimethylsilanediybis(9-fluorenyl))zirconium dichloride (**I**),⁸ a metallocene bearing an ansa ligand with all the steric requirements for suppressing chain-transfer reactions (Scheme 1), and its dimethyl derivative **II** (Chart 1). As a comparison we also prepared (ethylenebisfluorenyl)zirconium and -hafnium dichlorides (**III** and **IV**),¹⁴ which we expected to be less effective in increasing the molecular weight of polypro-



pylene. Propylene polymerization results⁸ (vide infra) show that, indeed, **I**/MAO and **II**/MAO produce aPP with the highest molecular weights so far observed among the metallocene class and that the Si bridge is superior with respect to the ethylene bridge in increasing the polymer molecular weights.

2. Synthesis and Characterization of the Ligands and the Zirconocenes. The synthesis of bis(9-fluorenyl)dimethylsilane¹⁵ followed the straightforward addition of a THF solution containing fluorene anion to a THF solution of Me_2SiCl_2 . The sequence of addition is critical in obtaining suitable yields. Crystals of the ligand were obtained as fine elongated colorless needles (5 mm \times 0.5 mm) when cooled from a concentrated solution of hot hexane.

The high-yield synthesis of $\text{Me}_2\text{Si}(9\text{-Flu})_2\text{ZrCl}_2$ (**I**) (Scheme 1) closely follows that developed for $\text{Me}_2\text{C}(\text{Me}_4\text{-Cp})(\text{Ind})\text{ZrCl}_2$ ¹⁶ and $\text{Et}(9\text{-Flu})_2\text{ZrCl}_2$ (**III**):¹⁴ a cold Et_2O suspension of $\text{Me}_2\text{Si}(9\text{-Flu})_2\text{Li}_2$ is added to a cold pentane slurry of ZrCl_4 , and the stirred mixture is then slowly allowed to warm to room temperature, while a deep red color develops. Simple filtration of the solids provides quantitative yields of **I**, which, being poorly soluble and quite unstable in all common organic solvents, could not be freed from $\text{LiCl}(\text{Et}_2\text{O})_x$. The presence of Et_2O is likely to lower catalytic activity. **I** is stable in dry air but extremely sensitive to moisture. The very simple synthetic procedures and ready availability of all starting materials render **I** a suitable catalyst precursor.

(9) Resconi, L.; Silvestri, R. In *The Polymeric Materials Encyclopedia*; Salamone, J. C., Ed.; CRC Press: Boca Raton, FL, in press.

(10) Stehling, U.; Diebold, J.; Kirsten, R.; Röhl, W.; Brintzinger, H. H.; Jüngling, S.; Mülhaupt, R.; Langhauser, F. *Organometallics* **1994**, *13*, 964–970.

(11) Ewen, J. In *Transition Metals and Organometallics as Catalysts for Olefin Polymerization*; Kaminsky, W., Sinn, H., Eds.; Springer-Verlag: Berlin 1988; pp 281–289.

(12) Tsutsui, T.; Mizuno, A.; Kashiwa, N. *Polymer* **1989**, *30*, 428–431. (b) Kaminsky, W.; Ahlers, A.; Möller-Lindenhof, N. *Angew. Chem., Int. Ed. Engl.* **1989**, *28*, 1216–1218.

(13) (a) Resconi, L.; Piemontesi, F.; Franciscono, G.; Abis, L.; Fiorani, T. *J. Am. Chem. Soc.* **1992**, *114*, 1025–1032. (b) Resconi, L.; Abis, L.; Franciscono, G. *Macromolecules* **1992**, *25*, 6814–6817.

(14) Alt, H.; Milius, W.; Palackal, S. *J. Organomet. Chem.* **1994**, *472*, 113–118. Synthesis of polypropylene with **III** and **IV** has been reported in the patent literature, but no polymer characterization had been reported: Alt, H.; Palackal, S.; Patsidis, K.; Welch, M.; Geerts, R.; Hsieh, E.; McDaniel, M.; Hawley, G.; Smith, P. Eur. Pat. Appl. 524 624 (to Phillips Petroleum), 1993.

(15) Sugimori, A.; Akiyama, T.; Kajitani, M.; Igarashi, H. *J. Pat. Appl.* 1,249,782 (to Mitsubishi Metal), 1989.

(16) Llinas, G. H.; Dong, S.-H.; Mallin, D. T.; Rausch, M. D.; Lin, Y.-G.; Winter, H. H.; Chien, J. C. W. *Macromolecules* **1992**, *25*, 1242.

Table 1. Crystallographic Data for $\text{Me}_2\text{Si}(\text{9-Flu})_2\text{ZrMe}_2$

(a) Crystal Data	
formula	$\text{C}_{30}\text{H}_{28}\text{SiZr}$
fw	507.8
cryst color and habit	orange block
cryst size, mm	$0.26 \times 0.34 \times 0.34$
cryst system	monoclinic
space group	$C2/c$
$a, b, c, \text{\AA}$	17.868(3), 9.944(2), 13.201(3)
β , deg	99.92(2)
$V, \text{\AA}^3$	2310.5(7)
Z	4
$D(\text{calc}), \text{g cm}^{-3}$	1.460
$\mu(\text{Mo K}\alpha), \text{cm}^{-1}$	5.44
(b) Data Collection	
diffractometer	Siemens P4 (Mo K α)
reflcs colld	2742 (max $2\theta = 55^\circ$)
indpdt reflcs	2625
obsd reflcs	1852 ($4\sigma(F)$)
(c) Refinement	
$R(F), R(wF)$, %	4.59, 5.95
data/param	12.7
$\Delta\rho(\text{max}), \text{e \AA}^{-3}$	0.74

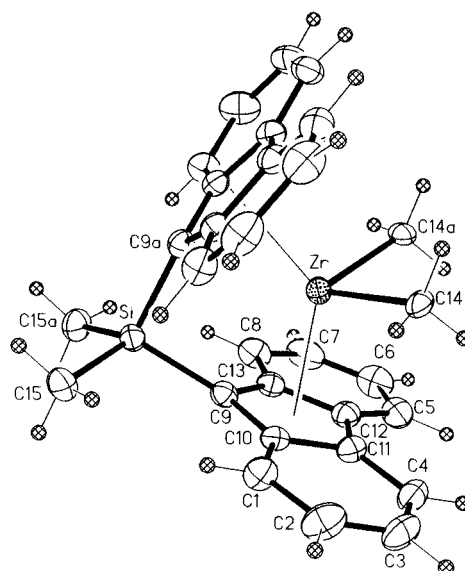
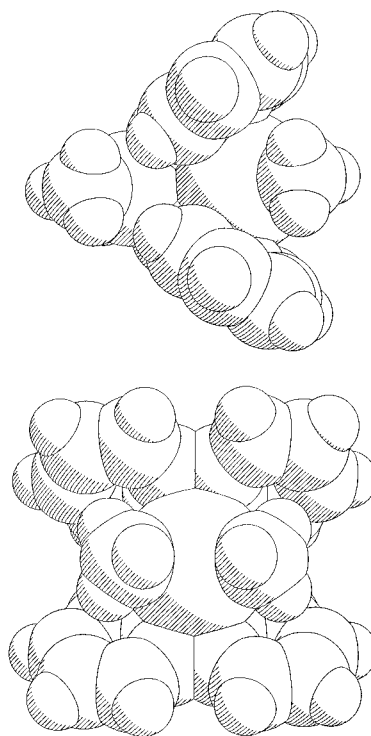
Table 2. Selected Bond Distances and Angles for $\text{Me}_2\text{Si}(\text{9-Flu})_2\text{ZrMe}_2$

(a) Bond Distances (\AA)			
Zr–cnt ^a	2.298(4)	C(10)–C(11)	1.433(6)
Zr–C(14)	2.336(4)	C(11)–C(12)	1.430(6)
Si–C(9)	1.857(4)	C(12)–C(13)	1.426(6)
Si–C(15)	1.848(5)	C(9)–C(13)	1.447(6)
C(9)–C(10)	1.446(6)	Zr–C(9)	2.442(4)
Zr–C(10)	2.557(4)	Zr–C(11)	2.712(4)
Zr–C(12)	2.722(5)	Zr–C(13)	2.567(5)
(b) Bond Angles (deg)			
cnt–Zr–cnt	130.3(1)	C(9)–Si–C(9a)	96.8(3)
cnt–Zr–C(14)	106.3(2)	C(9)–Si–C(15)	114.4(2)
cnt–Zr–C(14a)	106.7(2)	C(9)–Si–C(15a)	112.2(2)
C(14)–Zr–C(14a)	94.9(2)	C(15)–Si–C(15a)	106.9(3)

^a Centroid of C[9,10,11,12,13].

Attempts at preparing **I** following the standard protocol for bridged metallocenes¹⁷ of adding a THF solution of the ligand dianion to a cooled THF solution of ZrCl_4 or $\text{ZrCl}_4(\text{THF})_2$ resulted in little product formation. Methylene chloride¹⁸ proved to be less suitable for the metalation step. Methylation of **I** with MeMgBr in Et_2O produced $\text{Me}_2\text{Si}(\text{9-Flu})_2\text{ZrMe}_2$ (**II**). Filtration and recrystallization from CH_2Cl_2 afforded bright red crystals of **II**.

3. Crystal and Molecular Structure of $\text{Me}_2\text{Si}(\text{9-Flu})_2\text{ZrMe}_2$. $\text{Me}_2\text{Si}(\text{9-Flu})_2\text{ZrMe}_2$ (**II**) crystallizes in the monoclinic space group $C2/c$ with a crystallographically imposed 2-fold symmetry. Crystallographic data are collected in Table 1, while relevant molecular parameters are listed in Table 2. The molecular symmetry displayed in Figures 1 and 2 reveals nearly perfect C_{2v} symmetry. The angles defining the metal– π -ligand moiety are shown in Figure 3. The cnt–Zr–cnt angle (ϕ) (cnt = centroid), $130.3(2)^\circ$, is unusually large, as compared to the unbridged structures of $\text{Ind}_2\text{ZrMe}_2$, $120.8(5)^\circ$,¹⁹ and $(\text{9-Flu})_2\text{ZrCl}_2$, $125.0(4)^\circ$,²⁰ and the simi-

**Figure 1.** Molecular structure and labeling scheme for $\text{Me}_2\text{Si}(\text{Flu})_2\text{ZrMe}_2$ (**II**) drawn with 30% thermal ellipsoids.**Figure 2.** Space-filling depictions of $\text{Me}_2\text{Si}(\text{Flu})_2\text{ZrMe}_2$. The upper view is in the plane defined by the ring centroids and the Si and Zr atoms. The lower view is viewed along the Zr–Si axis.

larly bridged structure of $\text{Me}_2\text{Si}(\text{Cp})_2\text{ZrCl}_2$, $125.4(2)^\circ$,²¹ and $\text{Me}_2\text{Si}(\text{Ind})_2\text{ZrCl}_2$, $127.8(2)^\circ$.⁴ Correspondingly, the cnt–Zr distance in **II** is 0.1–0.2 \AA longer than those in the comparison structures. When the bridging group is made smaller by substituting CMe_2 for SiMe_2 , a smaller cnt–Zr–cnt angle is obtained, as might have been anticipated. In fact, in $\text{Me}_2\text{C}(\text{Cp})(\text{9-Flu})\text{ZrMe}_2$, the angle is only 119° ²² and most of the strain is absorbed in the bending (at γ , which could be seen as a strain-relief angle) of the bridge arms out of the plane of the coordinated five-membered ring. The smallest value for

(17) See for example: Grossman, R.; Doyle, R. A.; Buchwald, S. *Organometallics* **1991**, *10*, 1501. Lee, I.-M.; Gauthier, W.; Ball, J.; Iyengar, B.; Collins, S. *Organometallics* **1992**, *11*, 2115.

(18) Ewen, J.; Razavi, A. Eur. Pat. Appl. 351 392 (to Fina Technology), 1990.

(19) Atwood, J. L.; Hunter, W. E.; Hrcncir, D. C.; Samuel, E.; Alt, H.; Rausch, M. D. *Inorg. Chem.* **1975**, *14*, 1757.

(20) Kowala, C.; Wunderlich, J. A. *Acta Crystallogr.* **1976**, *B32*, 820.

(21) Bajgur, C. S.; Tikkanen, W. R.; Petersen, J. L. *Inorg. Chem.* **1985**, *24*, 2539.

Table 3. Comparison of Bonding Parameters for Four Bridged *ansa*-Zirconocenes^a

	av Zr–C(ring), Å	M–CNT, Å	X–M–X, deg	α , deg	β , deg	γ , deg	θ , deg	ϕ , deg
Me ₂ Si(Cp) ₂ ZrCl ₂ ^b	2.500	2.197	98.0	93.2	87.3	163.4	60.1	125.4
Me ₂ C(Cp) ₂ ZrMe ₂ ^c	2.511	2.210	100.8	99.0	86.8	165.8	71.8	115.6
C ₂ H ₄ (Flu) ₂ ZrCl ₂ ^d	2.574	2.269	96.9	N/A	83.4	173.3	64.3	129.0
Me ₂ Si(Flu) ₂ ZrMe ₂ ^e	2.600	2.298	94.9	96.8	82.0	165.3	65.6	130.3

^a Parameters are keyed to Figure 3. ^b Reference 21. ^c Reference 23. ^d Reference 14. ^e This work.

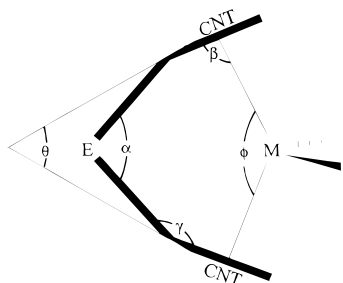


Figure 3. Schematic diagram of a bridged, C_{2v} -symmetric bent metallocene. CNT = centroid of the central five-membered ring, E = central element of the bridge, and M = metal atom.

ϕ , 115.6°, is observed in Me₂C(Cp)₂ZrMe₂²³ (γ = 165.8°). On the contrary, the longer bridge in **III** causes no bending of the bridge arms, and the ϕ value of 129.0°, similar to that of **II**, indicates that the larger ϕ and small γ observed in **II** are probably the result of repulsive effect of the four phenyl hydrogens in the four rear Cp positions α to the Me₂Si bridge.

The effect of the long cnt–Zr distance is to create greater accessibility to Zr, while a larger ϕ will likely decrease it. A complete analysis of the accessibility of the Zr atom for catalytic functions needs to consider another parameter, β , the deviation from perpendicularity of the Zr–cnt vector. Average Zr–C(ring) and Zr–Cp centroid distances and X–Zr–X α , β , γ , θ , and ϕ angles for four C_{2v} symmetric zirconocenes are compared in Table 3. Values of β near 90° result from equal Zr–C bonding around the cyclopentadienoid ring. Therefore, the value of β depends on the hapticity (η) of the Zr–ligand bond. Invariably, the Zr–C(ring) bond distances show a pattern of decreased hapticity for indenyl and fluorenyl ligands, the effect being greater for the fluorene. The longer the Zr–C(ring) bond distances, the weaker is the Zr–Cp bond reflecting the decreasing hapticity. Obviously, as ligand hapticity decreases, the reactivity of the metal atom increases. This accounts for the decreased stability toward hydrolysis of **I** and **II** versus Cp- and Ind-type zirconocenes, although no clear correlation with polymerization activities could be drawn (vide infra). In **II** the Zr–C distances show a clear distortion toward η^3 bonding (necessarily identically for both ligands). In the case of unbridged Flu₂ZrCl₂,²⁰ the two Flu ligands are sufficiently different to have been described as an η^5, η^3 system; one ring has Zr–C distance ranging from 2.40 to 2.81 Å, and the other, 2.40 to 2.65 Å. In **II**, the range is 2.44 to 2.74 Å which would indicate that the effect of the bridge is to

Table 4. Propylene Polymerization in Liquid Monomer at 50 °C with Selected Achiral Metallocene/MAO Catalysts^a

sample	metallocene	g_{PP} , mmol _M ·h	\bar{P}_n^b
1	Cp ₂ ZrCl ₂	5 700	17
2	Cp ₂ HfCl ₂	4 600	140
3	(MeCp) ₂ ZrCl ₂	24 500	35
4	Cp* ₂ ZrCl ₂	3 600	4.5
5	Cp* ₂ HfCl ₂	12 600	3.4
6	Ind ₂ ZrCl ₂	18 300	100
7	Me ₂ Si(Cp) ₂ ZrCl ₂	9 100	17
8	Me ₂ Si(Me ₄ Cp) ₂ ZrCl ₂	3 700	300
9	EtFlu ₂ ZrCl ₂	20 000	1700 ^c
10	EtFlu ₂ HfCl ₂	9 000 ^d	1600 ^c
11	Me ₂ SiFlu ₂ ZrCl ₂	16 000 ^d	4700 ^c
12	Me ₂ SiFlu ₂ ZrMe ₂	29 000 ^d	3800 ^c

^a Polymerization conditions: 1-L or 2-L stainless-steel autoclave, 0.5 or 1 L liquid propylene, 50 °C, 1 h, Al/Zr ratio 1000, metallocene/MAO solutions aged in toluene (10–20 mL) for 5–10 min at room temperature. ^b \bar{P}_n = number-average polymerization degree from ¹H NMR (assuming 1 double bond per chain). ^c \bar{P}_n from intrinsic viscosity²⁹ assuming M_w/M_n = 2. ^d Al/Zr = 2000.

create two rings that are intermediate to an untethered system.

4. Propylene Polymerization. As previously discussed, **I** was our metallocene precatalyst of choice for the synthesis of high-molecular-weight atactic polypropylene. Propylene polymerization results (liquid monomer conditions, MAO as cocatalyst, 50 °C) for **I** and its methylated derivative **II** in comparison to other C_{2v} -symmetric aspecific metallocenes are reported in Table 4. All zirconocenes and hafnocenes give lower molecular weights than **I** and **II**. The bulky fluorenyl ligands do not lower catalyst activity to a large extent, although activities for these systems are much lower compared to the best isospecific systems.^{1b,10} The ethylene bridged zirconocene **III**, although of activity comparable to **I** and **II**, gives lower molecular weight polypropylenes than the latter, as does the hafnocene **IV**. The reasons for this behavior is discussed in the section on chain transfer mechanisms (vide infra).

Samples 1–8 are liquids or viscous oils, while 9 and 10 are sticky solids and 11 and 12 are nonsticky, elastomeric materials. All products are soluble in ether, hydrocarbons, and chlorinated solvents, although solubility decreases with increasing molecular weight.

¹³C NMR analysis confirms that, at this polymerization temperature, the C_{2v} -symmetric metallocenes produce atactic or nearly atactic oligo- or polypropylenes and the polymerization mechanism is Bernoullian in all cases. All samples, with the exception of sample 6,^{13b} are highly regioregular, as no head-to-head to tail-to-tail propylene units could be detected.

The methyl pentad region of aPP sample 11 is reported in Figure 4. It can be observed that 11 is slightly syndiotactoid (rde = 17%,^{13b} rrrr = 3.6 mmmm). A Bernoullian index of 1.0 indicates that a weak syndiospecific chain end control^{13b,24} is operating with **I**.

(22) Ewen, J. A.; Elder, M. J.; Jones, R. L.; Curtis, S.; Cheng, H. N. *Proc. Int. Symp. Recent Dev. Olefin Polym. Catal. Tokyo* **1989**, 439. Ewen, J. A.; Elder, M. J.; Jones, R. L.; Haspelslagh, L.; Atwood, J.; Bott, S.; Robinson, K. *Makromol. Chem., Macromol. Symp.* **1991**, 48/49, 253.

(23) Nifant'ev, I. E.; Churakov, A. V.; Urazowski, I. F.; Mkoyan, Sh. G.; Atovmjan, L. O. *J. Organomet. Chem.* **1992**, 435, 37.

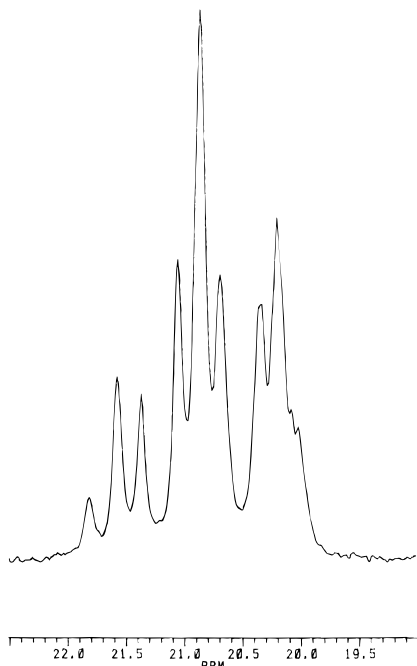


Figure 4. ^{13}C NMR pentad region for sample 11: mm 16.83%, mr 48.55%, rr 34.62%. Bernoullian factor $B = 0.99$.

The chain transfer mechanisms operating with a given catalyst can be established from NMR end-group analysis of the propylene polymers, provided their molecular weight is sufficiently low. Besides β -hydrogen transfer, which can be monomolecular or first order in monomer concentration (chain-transfer to the monomer),¹⁰ two other chain-transfer reactions have been detected for group 4 metallocene/MAO and related cationic catalysts: transfer to the Al cocatalyst²⁵ and transfer via β -methyl elimination.^{13a,26}

The latter has been found to be the major cause for molecular weight depression only with $(\text{Me}_5\text{Cp})_2\text{M}$ - and, to a lower extent, with $(\text{Me}_4\text{Cp})_2\text{M}$ -type catalysts^{26d} ($\text{M} = \text{Zr}, \text{Hf}$), i.e. having rather large ($\approx 135^\circ$) $\text{Cp}-\text{M}-\text{Cp}$ angles and extensive Cp alkylation. Chain transfer to aluminum has been observed only at high Al/M ratios or at relatively low polymerization temperatures. For polymerizations carried out at 50°C in liquid propylene, and at $\text{Al}/\text{M} \leq 2000$, this transfer reaction is generally below detectability.^{13a} With **I**, however, chain transfer to Al appears to be an accessible (although minor) chain transfer pathway, as molecular weights are lower at higher MAO/Zr ratios.⁹

The higher molecular weights of samples 9–12 prevented the observation of end groups in their ^1H -NMR spectra. In order to gain more insight into the polym-

Table 5. Chain-Transfer Mechanisms with Different Zirconocenes^a

sample	metallocene	T_p	β -Me	β -H	\bar{P}_n
13	$\text{Ind}_2\text{ZrCl}_2$	50	100		45
14	$\text{Flu}_2\text{ZrCl}_2$	50	68	31	190
15	$\text{EtFlu}_2\text{ZrCl}_2$	50	75	25	315
16	$\text{Me}_2\text{SiFlu}_2\text{ZrCl}_2$	50	n.d.	n.d.	1500
17	$\text{Me}_2\text{SiFlu}_2\text{ZrCl}_2$	80	82	18	70

^a As determined from the structure of the olefinic end groups.^{13a} Polymerization conditions: 4 bar-a, 0.4 L *n*-hexane, [propylene] = 1.7₆ mol/L (samples 13–16), or 100 mL of toluene [propylene] = 2.8 mol/L (sample 17), Al/Zr ratio 2000, 1 h. \bar{P}_n = number-average polymerization degree from ^1H NMR (assuming 1 double bond per chain) or GPC.

erization mechanism with **I–IV**, polymerizations were run at 50°C and lower monomer concentration. The results are reported in Table 5. Both **III** and **IV** show predominance of allylic end groups (allyl:vinylidene = 75:25) in their proton spectra, the signature of β -methyl transfer. The lower selectivity of **III** and **IV** toward β -methyl transfer compared to $\text{Cp}^*_2\text{ZrCl}_2$ and $\text{Cp}^*_2\text{HfCl}_2$ reflects the lower steric hindrance of sp^2 carbons versus methyl groups and the smaller $\text{Cp}-\text{M}-\text{Cp}$ angle ($135-138^\circ$ for $\text{Cp}^*_2\text{ZrR}(\text{L})^+$ ^{26b,27} versus 129° for **III**¹⁴) caused by the bridge. The much higher molecular weights indicate that in **III** and **IV** there is a competition between the effect of fluorenyl (increase in molecular weight, likely electronic in nature) and that of the catalyst geometry (favoring β -methyl transfer, hence lowering molecular weights).

Despite lower monomer concentrations, the molecular weight of aPP sample 16 prepared with **I**/MAO was still too high for end group determination, again confirming the depression of chain transfer reaction rates caused by the $\text{Me}_2\text{SiFlu}_2$ system. Polymerization of propylene at 80°C in toluene at 3 bar finally provided a low molecular weight sample ($\bar{M}_n = 3000$) for which the end group structure was determined to be 82:18 = allyl:vinylidene. The unsaturated end group region of the proton spectra (CDCl_3 , room temperature) of 4-methyl-1-pentene (a), sample 5 (b), sample 17 (c), sample 15 (d), and sample 1 (e) are reported in Figure 5.

These findings show that there is a close similarity between the ethylenebis(fluorenyl) and dimethylsilylanediylbis(fluorenyl) ligands in the selection of chain transfer modes. The higher aPP molecular weights provided by **I** and **II** with respect to those obtained with **III** and **IV** (assuming similar amounts of active centers, as indicated by the similar activities, at least for **I–III**) could be due to electronic rather than steric effects caused by the presence of the electron-releasing dimethylsilyl moiety,²⁸ as there appears to be no relevant differences in the geometric parameters of **II** and **III**.

In order to obtain a deeper understanding of the mechanism of chain transfer with **I**, a series of polymerization experiments were carried out at 50°C at different monomer concentrations (Table 6).

We³⁰ have recently shown that for isospecific metallocene catalysts affected by epimerization, and for which two chain transfer mechanisms involving β -hydrogen transfer (that is hydrogen transfer to the metal, $R_{\text{tMet}} =$

(24) Erker, G.; Fritze, C. *Angew. Chem., Int. Ed. Engl.* **1992**, *31*, 199.

(25) (a) Chien, J. C. W.; Wang, B. P. *J. Polym. Sci., A: Polym. Chem.* **1988**, *26*, 3089. (b) Chien, J. C. W.; Razavi, A. *J. Polym. Sci., A: Polym. Chem.* **1988**, *26*, 2369. (c) Chien, J. C. W.; Wang, B. P. *J. Polym. Sci., A: Polym. Chem.* **1990**, *28*, 15. (d) Resconi, L.; Bossi, S.; Abis, L. *Macromolecules* **1990**, *23*, 4489–4491.

(26) (a) Eshuis, J.; Tan, Y.; Teuben, J. H.; Renkema, J. *J. Mol. Catal.* **1990**, *62*, 277. (b) Eshuis, J.; Tan, Y.; Meetsma, A.; Teuben, J. H. *Organometallics* **1992**, *11*, 362. (c) Yang, X.; Stern, C. L.; Marks, T. *J. Angew. Chem., Int. Ed. Engl.* **1992**, *31*, 1375. (d) Mise, T.; Kageyama, A.; Miya, S.; Yamazaki, H. *Chem. Lett.* **1991**, 1525. (e) Kesti, M.; Waymouth, R. *J. Am. Chem. Soc.* **1992**, *114*, 3565. (f) Guo, Z.; Swenson, D.; Jordan, R. *Organometallics* **1994**, *13*, 1424. (g) Hajela, S.; Bercaw, J. E. *Organometallics* **1994**, *13*, 1147. (h) Yang, X.; Stern, C. L.; Marks, T. *J. Am. Chem. Soc.* **1994**, *116*, 10015.

(27) Amorose, D.; Lee, R.; Petersen, J. *Organometallics* **1991**, *10*, 2191. Hlatky, G.; Turner, H.; Eckman, R. *J. Am. Chem. Soc.* **1989**, *111*, 2728.

(28) Gassman, P. G.; Deck, P. A.; Winter, C. H.; Dobbs, D. A.; Cao, D. H. *Organometallics* **1992**, *11*, 959.

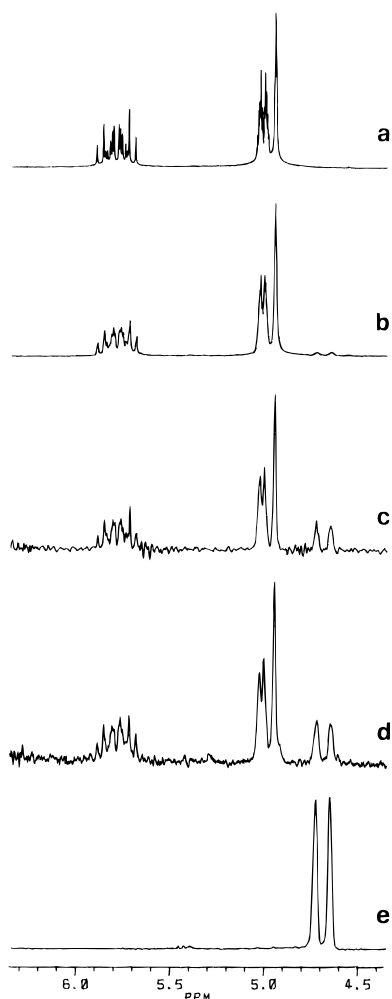


Figure 5. Unsaturated end group region of the proton spectra (200 MHz, CDCl_3 , room temperature) of 4-methyl-1-pentene (a), sample 5 (b), sample 17 (c), sample 15 (d), and sample 1 (e).

$k_{t_{\text{Met}}}[\text{C}^*]$, and hydrogen transfer to the monomer, $R_{t_{\text{Mon}}} = k_{t_{\text{Mon}}}[\text{C}^*][\text{M}]$) can occur, the number average degree of polymerization varies with [propylene] according to eq 1.

$$\bar{P}_n = \frac{K'_{p_1}[\text{M}] + K'_{p_2}[\text{M}]^2}{K'_{t_{\text{Met}}} + K'_{t_1}[\text{M}] + K'_{t_2}[\text{M}]^2} \quad (1)$$

In the case of aspecific metallocene catalysts, eq 1 reduces to eq 2. The weight average molecular weights

$$\bar{P}_n = \frac{k_p[\text{M}]}{k_{t_{\text{Met}}} + k_{t_{\text{Mon}}}[\text{M}]} \quad (2)$$

for samples 18–23, as obtained by their intrinsic viscosities and the Mark–Houwink–Sakurada parameters derived by Pearson and Fetters²⁹ and assuming $\bar{M}_w/\bar{M}_n = 2$ for all samples (experimental values for selected samples are in the 2–2.2 range), are listed in

Table 6. Effect of Monomer Concentration on the Molecular Weight of aPP Made with $\text{Me}_2\text{SiFlu}_2\text{ZrCl}_2/\text{MAO}^a$

sample	[M], mol/L	activity, g/mmol	$[\eta]^b$, dL/g	\bar{M}_w^c	\bar{P}_n^d
18	0.7 ₃	1300	0.87	96 100	1142
19	1.2 ₄	3700	1.16	142 000	1687
20	1.7 ₆	7600	1.30	165 800	1970
21	2.2 ₈	8300	1.61	221 600	2633
22	2.8 ₃	9600	1.80	257 800	3063
23 ^e	10.5 ₆	11200	2.67	440 200	5230

^a Polymerization conditions: 1-L Büchi glass autoclave, 50 °C, 1 h, stirring rate 800 rpm, catalyst $\text{Me}_2\text{SiFlu}_2\text{ZrCl}_2$ (2–4 mg)/MAO solutions aged in 10 mL of toluene for 10 min at room temperature, Al/Zr ratio 1200, 400 mL of n-hexane. ^b Intrinsic viscosity measured at 135 °C in THN. ^c Estimated from the $[\eta] = 1.85 \times 10^{-4} \bar{M}_w^{0.737}$; see ref 29. ^d Estimated assuming $\bar{M}_w/\bar{M}_n = 2$. ^e Polymerization in liquid monomer.

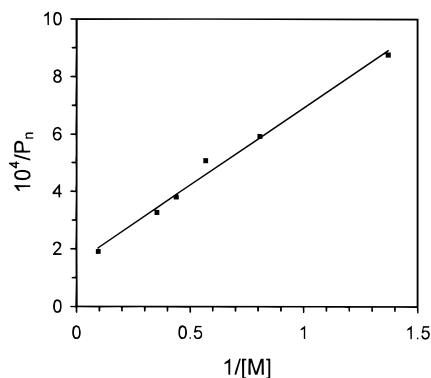


Figure 6. $1/\bar{P}_n$ versus $1/[\text{propylene}]$ plot for I/MAO at 50 °C in propylene/hexane mixtures: $R = 0.995$; slope 5.374; intercept 1.54.

Table 6. These values obey the linear form of eq 2

$$\frac{1}{\bar{P}_n} = \frac{k_{t_{\text{Mon}}}}{k_p} + \frac{k_{t_{\text{Met}}}}{k_p} \frac{1}{[\text{M}]} \quad (3)$$

in the whole range of monomer concentrations (Figure 6). Assuming chain transfer to aluminum to be negligible in our polymerization conditions, the obtained values of $k_{t_{\text{Mon}}}/k_p = 1.54 \times 10^{-4}$ and $k_{t_{\text{Met}}}/k_p = 5.37 \times 10^{-4}$ give a $k_{t_{\text{Met}}}/k_{t_{\text{Mon}}}$ ratio of 3.5; i.e., bimolecular chain transfer equals 22% of all transfer reactions. Assuming that the $\beta\text{-H}/\beta\text{-CH}_3$ ratio observed at 80 °C ($\beta\text{-H} = 18\%$; see Table 5) is the same also at 50 °C, it seems reasonable to assign bimolecular chain transfer to β -hydrogen transfer (hydrogen transfer to the monomer) and monomolecular chain transfer to β -methyl transfer (methyl transfer to the metal). From the polymerization activities listed in Table 6, assuming that average productivities are good representative of instant catalyst activities, an approximate first-order dependence of propagation rate on monomer concentration can be observed in the range 0.7–2.8 mol/L. The loss of activity in liquid monomer is likely associated with the insolubility of aPP in propylene, generating catalyst trapping and monomer diffusion problems.

Conclusions

By the proper selection of the π -ligands, we have designed a zirconocene catalyst which produces high-molecular-weight, regioregular atactic polypropylene: a novel propylene polymer whose physical properties and possible applications are currently under investigation

(29) Pearson, D.; Fetters, L.; Younghouse, L.; Mays, J. *Macromolecules* **1988**, *21*, 478.

(30) Resconi, L.; Fait, A.; Piemontesi, F.; Colonna, M.; Rychlicki, H.; Zeigler, R. *Macromolecules* **1995**, *28*, 6667.

in our laboratories. The molecular and crystal structure of one of the selected zirconocenes, $\text{Me}_2\text{SiFlu}_2\text{ZrMe}_2$, has been reported. By comparison between the geometries of different C_{2v} - or pseudo- C_{2v} -symmetric zirconocene catalyst precursors and the type and extent of chain transfer reactions occurring in propylene polymerization with the corresponding zirconocene/MAO catalysts, a better understanding of the metallocene structure/chain transfer mechanism relationship has been achieved. In particular, we have provided two additional examples of persubstituted Cp ligands triggering β -methyl elimination. The latter seems to be a unimolecular reaction and now appears to be a more general chain transfer mechanism than previously realized.

Experimental Section

General Procedures. All operations were performed under nitrogen by using conventional Schlenk-line techniques. Solvents were distilled from LiAlH_4 (THF, Et_2O), P_4O_{10} (CH_2Cl_2 , CHCl_3), or $\text{Al}(\text{i-Bu})_3$ (toluene, hexane, pentane), and stored under nitrogen. Typical residual water content was 2 ppm. Polymerization grade propylene was received directly from the Montell Ferrara plant. ZrCl_4 , HfCl_4 , fluorene, Me_2SiCl_2 , and 1,2-dibromoethane (Aldrich) were used as received. MAO was a commercial product (Witco, 30% w/w in toluene) treated as previously recommended in order to remove most of the unreacted TMA.^{25d} The chemical purities of all compounds were confirmed by $^1\text{H NMR}$ (200 MHz, CDCl_3 , signal-to-noise ratio 200).

Polymerizations. Polymerizations were carried out in either a 1-L Büchi glass autoclave (solution polymerizations with continuous monomer feed) or a 2-L stainless-steel autoclave (liquid monomer polymerizations) at constant pressure for 1 h and 50 (± 1) °C. Nitrogen was eliminated by purging the system for several minutes. Stirring was kept at 800 rpm by means of a three-blade propeller. Metallocene and MAO were precontacted for 10 min in toluene solution (10 mL) and then added to the monomer/solvent mixture at 48 °C. The polymerizations were quenched with CH_3OH ; the polymers were isolated by distilling off the solvents under reduced pressure and then washed with either acetone or CH_3OH and dried at 50 °C in vacuo overnight.

Polymer Analysis. Intrinsic viscosities were measured at 135 °C in THN. GPC measurements were carried out on a Waters 150-C GPC equipped with TSK columns (Model GM-HXL-HT) at 135 °C with 1,2-dichlorobenzene as solvent. Monodisperse fractions of polystyrene were used as a standard. $^{13}\text{C NMR}$ spectra were obtained on a Bruker AC 200 working at 50.323 MHz at 120 °C in nonspinning, broad-band decoupling mode, using a 45° pulse width (4.8 μs), 10 s relaxation delay, and 10 000–15 000 transients for each sample. For end group quantitative evaluation, the spectra (25 000 transients) were acquired with the INVGATE sequence under the same experimental conditions.

Synthesis of the Ligands and the Metallocenes. Dimethylbis(9-fluorenyl)silane. Fluorene (50 g, 300 mmol) was dissolved in 350 mL of THF, and the solution was cooled to 0 °C with an ice bath. *n*-Butyllithium (2.5 M in hexane, 120 mL) was added dropwise to the stirred solution while the temperature was maintained at 0 °C. After the addition was complete, the solution was warmed to room temperature and stirring was continued for 5 h after gas evolution had ceased. The resulting solution was then added dropwise to a stirred solution of Me_2SiCl_2 (19.4 g, 150 mmol) in THF (150 mL), maintained at 0 °C during the addition. After the addition was complete, the solution was warmed to room temperature and stirred for 14 h. The reaction was quenched with water and the organic phase collected and dried over MgSO_4 . Solvents were removed in vacuo, and the solids collected were recrystallized from hot hexane, yielding 37 g (63%) of dimeth-

ylbis(9-fluorenyl)silane. $^1\text{H NMR}$ (CD_2Cl_2 , δ , ppm): 7.9 (d, 4H), 7.6 (d, 4H), 7.4 (t, 4H), 7.3 (t, 4H), 4.3 (s, 2H), -0.5 (s, 6H).

Bis(9-fluorenyl)ethane.¹⁴ Fluorene (50 g, 300 mmol) was dissolved in 350 mL of THF, and the solution was cooled to 0 °C with an ice bath. *n*-Butyllithium (2.5 M in hexane, 120 mL) was added dropwise to the stirred solution while the temperature was maintained at 0 °C. After the addition was complete, the solution was warmed to room temperature and stirred for 5 h after gas evolution had ceased. The solution was then cooled to -78 °C, and 1,2-dibromoethane (28.3 g, 150 mmol) was added dropwise to the stirred solution. After the addition was complete, the reaction mixture was warmed to room temperature and stirred overnight. The reaction was then quenched with 250 mL of saturated aqueous NH_4Cl , and the organic phase was collected and dried over MgSO_4 . Solvents were removed in vacuo yielding 34.6 g of bis(9-fluorenyl)ethane (64.3%). $^1\text{H NMR}$ (CDCl_3 , δ , ppm): 1.75 (m, 4H), 3.85 (broad s, 2H), 7.1–7.5 (m, 12H), 7.73–7.77 (d, 4H).

Bis(9-fluorenyl)zirconium Dichloride ($\text{Flu}_2\text{ZrCl}_2$).²⁰ Fluorene (10 g) was dissolved in 50 mL of dimethoxyethane, and 2.41 g of KH was added as a dry powder to the stirred solution at room temperature. The reaction mixture was stirred overnight and then added dropwise to a stirred solution of ZrCl_4 (7.0 g) in 20 mL of dimethoxyethane. After 2 h, Et_2O was added to precipitate the product. The solids were then collected by filtration, washed with fresh Et_2O , and finally dried in vacuo, yielding 14.78 g of an orange powder containing $\text{KCl}(\text{Et}_2\text{O})_x$.

(Dimethylsilanediylbis(9-fluorenyl))zirconium Dichloride ($\text{Me}_2\text{SiFlu}_2\text{ZrCl}_2$). Dimethylbis(9-fluorenyl)silane (8.5 g, 21.9 mmol) was dissolved in 150 mL of Et_2O . Methylolithium (1.4 M in Et_2O , 32.5 mL) was added dropwise to the rapidly stirred solution, which was maintained at 0 °C during the addition. After the addition was complete, the mixture was warmed to room temperature and stirred for 5 h after gas evolution had ceased. The resulting suspension was cooled to -78 °C and then added to a rapidly stirred slurry of ZrCl_4 (5.1 g, 21.9 mmol) in pentane (150 mL) also maintained at -78 °C. After the addition was complete, the reaction mixture was slowly warmed to room temperature and stirred overnight. Solvents were then removed by filtration, and the solids collected were washed with Et_2O and then pentane. The bright red complex was dried to a free-flowing powder under vacuum at room temperature. Yield: 13.1 g. The purity of the complex (85% by weight) was measured by elemental analysis, acidic decomposition, GC-MS analysis of the CHCl_3 solubles, and $^1\text{H NMR}$. $^1\text{H NMR}$ (CD_2Cl_2 , δ , ppm): 7.9 (d, 4H), 7.8 (d, 4H), 7.4 (t, 4H), 7.1 (t, 4H), 1.6 (s, 6H).

(Dimethylsilanediylbis(9-fluorenyl))zirconium Dimethyl ($\text{Me}_2\text{SiFlu}_2\text{ZrMe}_2$). (Dimethylsilanediylbis(9-fluorenyl))zirconium dichloride (6.0 g) was suspended in 50 mL of Et_2O . Methylmagnesium bromide (7.29 mL of a 3.0 M solution in Et_2O) was added dropwise to the rapidly stirred slurry, which was maintained at 0 °C during the addition. After addition was complete, the mixture was allowed to warm to room temperature and stirred overnight. The solids were collected by filtration, washed with Et_2O and pentane, and finally dried under vacuum. A yield of 6.5 g of product was obtained. $^1\text{H NMR}$ (300 MHz, CD_2Cl_2 , δ , ppm): 7.9 (d, 4H), 7.7 (d, 4H), 7.2 (t, 4H), 7.0 (t, 4H), 1.4 (s, 6H), -2.5 (s, 6H).

(Ethylenebis(9-fluorenyl))zirconium Dichloride ($\text{EtFlu}_2\text{ZrCl}_2$).¹⁴ Bis(9-fluorenyl)ethane (3.58 g, 10 mmol) was suspended in 150 mL of Et_2O . Methylolithium (1.4 M in Et_2O , 14.3 mL) was added dropwise to the rapidly stirring mixture, which was maintained at 0 °C during the addition. After the addition was complete, the mixture was warmed to room temperature and stirring continued for 17 h after gas evolution had ceased. The resulting suspension was cooled to -78 °C and then added to a rapidly stirring slurry of ZrCl_4 (2.33 g, 10 mmol) in pentane (100 mL) at -78 °C. After the addition was complete, the reaction mixture was allowed to warm to room temperature. Solvents were then removed by filtration, and the solids

collected were washed with Et₂O and then pentane. The light red complex was dried to a free-flowing powder under vacuum at room temperature. Yield: 5.4 g.

(Ethylenebis(9-fluorenyl)hafnium Dichloride (EtFlu₂HfCl₂)).¹⁴ Bis(9-fluorenyl)ethane (7.2 g, 20 mmol) was suspended in 150 mL of Et₂O. Methylolithium (1.4 M in Et₂O, 28.7 mL) was added dropwise to the rapidly stirring mixture, which was maintained at 0 °C during the addition. After the addition was complete, the mixture was warmed to room temperature and stirring continued for 17 h after gas evolution had ceased. The solids were collected by filtration, washed with Et₂O, and resuspended in Et₂O. The resulting slurry was then cannulated dropwise into a rapidly stirring suspension of HfCl₄ (7.0 g, 21.8 mmol) in pentane (100 mL) at -78 °C. After the addition was complete, the reaction mixture was slowly warmed to room temperature. Solvents were then removed by filtration, and the solids collected were washed with Et₂O and then pentane. The bright orange complex was dried to a free-flowing powder under vacuum at room temperature. Yield: 10.93 g.

X-ray Structural Determination of Me₂SiFlu₂ZrMe₂. Crystallographic data are collected in Table 1. A specimen mounted in a glass capillary was determined photographically to possess 2/m Laue symmetry. Systematic absences in the diffraction data indicated either of the space groups *Cc* or *C2/c*. The latter, centrosymmetric choice was originally chosen

due to the frequency with which symmetrically substituted bent metallocene structures incorporate crystallographic 2-fold symmetry; it was later confirmed by the results of refinement. No correction for absorption was required. The structure was solved by direct methods. All non-hydrogen atoms were refined anisotropically, and hydrogen atoms were treated as idealized, updated contributions. All computations used the SHELXTL (4.2) program library (G. Sheldrick, Siemens XRD, Madison, WI).

Acknowledgment. We thank M. Colonna for the polymerization experiments, I. Camurati for the NMR spectra, F. Testoni for the GC-MS analysis, and T. Orr for her skilled technical assistance. We are indebted to Dr. A. Fait for evaluating the monomer concentrations in the hexane-propylene system.

Supporting Information Available: A plot of propylene concentration in the propylene/hexane system at 50 °C and tables of crystallographic data, bond distances, bond angles, anisotropic thermal parameters, and complete atom coordinates and thermal parameters (8 pages). Ordering information is given on any current masthead page.

OM950197H